Journal of Molecular Structure 1085 (2015) 155–161

Contents lists available at ScienceDirect

Journal of Molecular Structure

journal homepage: www.elsevier.com/locate/molstruc

Synthesis, crystal structure, theoretical calculations and antimicrobial properties of [Pt(tetramethylthiourea)$_4$] [Pt(CN)$_4$]·4H$_2$O

Haseeba Sadaf [a], Anvarhusein A. Isab [b], Saeed Ahmad [a,*], Arturo Espinosa [c,*], Míriam Mas-Montoya [c], Islam Ullah Khan [d], Ejaz [d], Seerat-ur Rehman [a], Muhammad Akhtar Javed Ali [a], Muhammad Saleem [e], José Ruiz [f,*], Christoph Janiak [g]

[a] Department of Chemistry, University of Engineering and Technology, Lahore 54890, Pakistan
[b] Department of Chemistry, King Fahd University of Petroleum and Minerals, Dhahran 31261, Saudi Arabia
[c] Department of Organic Chemistry, Faculty of Chemistry, Campus de Espinardo, University of Murcia, 30071 Murcia, Spain
[d] Department of Chemistry, Government College University, Lahore 54000, Pakistan
[e] Department of Civil Engineering, Jubail University College, P. O. Box 10074, Jubail Industrial City 31961, Saudi Arabia
[f] Department of Inorganic Chemistry, Faculty of Chemistry, Campus de Espinardo, University of Murcia and Instituto Murciano de Investigación Biosanitaria, 30071 Murcia, Spain
[g] Institut für Anorganische Chemie und Strukturchemie, Heinrich-Heine-Universität Düsseldorf, Universität-Str. 1, 40204 Düsseldorf, Germany

HIGHLIGHTS

- The synthesis and crystal structure of [Pt(Tmtu)$_4$][Pt(CN)$_4$] is presented.
- Homodromic H-bonds of four H$_2$O molecules per unit cell determine a 2D-network.
- Complex [Pt(Tmtu)$_4$][Pt(CN)$_4$] is moderately active against some microorganisms.
- Possible intermediacy of [Pt(Tmtu)$_2$(CN)$_2$)] is evaluated by DFT calculations.
- Complex [(Tmtu)$_2$Pt(μ^2-CN)(μ^2-η^2-CN)Pt(Tmtu)(CN)]CN was identified and characterized.

GRAPHICAL ABSTRACT

A new dinuclear platinum(II) complex formed by a [Pt(Tmtu)$_4$]$^{2+}$ cation (Tmtu = tetramethylthiourea) and a [Pt(CN)$_4$]$^{2-}$ anion is described and its higher stability with respect to a dimeric heterocoordinated [Pt(Tmtu)$_2$(CN)$_2$)] species computationally evaluated.

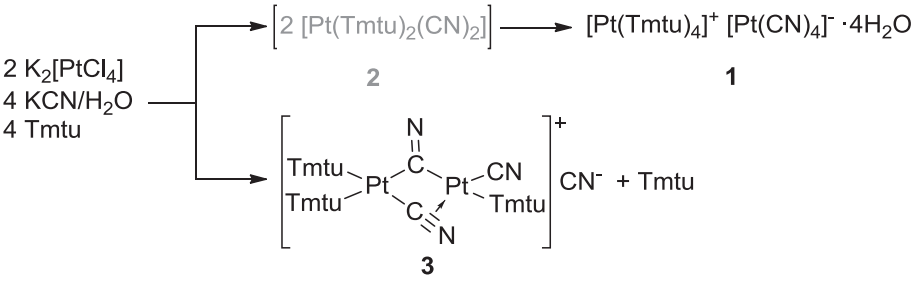

ARTICLE INFO

Article history:
Received 19 November 2014
Received in revised form 25 December 2014
Accepted 26 December 2014
Available online 5 January 2015

Keywords:
Platinum(II) complexes
Tetramethylthiourea
Cyanide
DFT calculations
X-ray structure

ABSTRACT

A new platinum(II) complex, [Pt(Tmtu)$_4$][Pt(CN)$_4$]·4H$_2$O (**1**) was synthesized by reaction of K$_2$[PtCl$_4$], KCN and tetramethylthiourea (Tmtu). Its structure was determined by X-ray crystallography. The [Pt(CN)$_4$]$^{2-}$ anion shows regular square planar geometry at platinum, while in the [Pt(Tmtu)$_4$]$^{2+}$ cation the geometry at platinum is somewhat distorted. Hydrogen bonding between water molecules and the cyanide nitrogen of [Pt(CN)$_4$]$^{2-}$ ions stabilizes the structure and leads to a supramolecular 2D network. DFT calculations support the experimentally found dinuclear (homocoordinated) ion-pair structure **1** as the most stable in comparison to noncovalent dimer [Pt(CN)$_2$(Tmtu)$_2$]$_2$ **2$_2$** that could, in turn, be involved in the formation sequence of **1**. Antimicrobial activities of the complex were evaluated by minimum inhibitory concentration and the results showed that the complex exhibited moderate activities against gram-negative bacteria (*Escherichia coli*, *Pseudomonas aeruginosa*) and molds (*Aspergillus niger, Penicillium citrinum*).

* Corresponding authors. Tel.: +92 333 5248570 (S. Ahmad). Tel.: +34 868 88 7489; fax: +34 868 88 4149 (A. Espinosa). Tel.: +34 868 88 74 55; fax: +34 868 88 4148 (J. Ruiz).
E-mail addresses: saeed_a786@hotmail.com (S. Ahmad), artuesp@um.es (A. Espinosa), jruiz@um.es (J. Ruiz).
URLs: http://www.um.es/multipropchem/artuesp (A. Espinosa), http://www.um.es/qcqo/jruiz.htm (J. Ruiz).

http://dx.doi.org/10.1016/j.molstruc.2014.12.076
0022-2860/

Introduction

Platinum compounds represent the most effective and widely used anticancer drugs [1,2]. However, their use is restricted because of the severe side effects and due to drug resistance caused by the platinum binding to biological thiolate molecules [2–4]. Thiourea and its derivatives are among such S-donor ligands that are used as chemoprotectants against nephrotoxicity after cisplatin treatment [4,5]. Several platinum(II) complexes of thioureas are also known to exhibit antibacterial and antitumor activity [6]. In addition, $[Pt(thiourea)_4]^{+2}$ complexes have been found suitable as molecular building blocks in the synthesis of hydrogen bonding networks [7]. Considering the above mentioned facts crystal structures of several platinum(II) complexes of thioureas have been reported in the literature [7,8]. The coordination of soft platinum(II) ion to thioureas in these compounds occurs through the softer sulfur atom [7,8].

In this paper, we present the crystal structure and biological properties of a new platinum(II) complex with tetramethylthiourea (Tmtu) and cyanide as ligands, $[Pt(Tmtu)_4][Pt(CN)_4]\cdot 4H_2O$ (**1**), together with experimental and theoretical support for explaining its formation. The spectroscopic data and theoretical structure of another new complex, $[Pt_2(CN)_3(Tmtu)_3]CN$ (**3**), is also presented.

Results and discussion

Synthesis and spectroscopic characterization

The sequential reaction of $K_2[PtCl_4]$ with KCN and Tmtu in a 1:2:2 M ratio resulted in a final product **1** of empirical composition $Pt(Tmtu)_2(CN)_2\cdot 2H_2O$ (Scheme 1). In the IR spectrum of **1** characteristic bands for coordinated Tmtu were observed: ν(C═S) at 607 cm^{-1} and ν(C—N) at 1561 cm^{-1}. For the free Tmtu these bands were observed at 622 and 1491 cm^{-1}, respectively [9]. The cyanide CN stretching frequency at 2128 cm^{-1} is close to that observed for the $[Pt(CN)_4]^{2-}$ ion [10]. The ν(O—H) vibration appeared at 3400 cm^{-1} showing the presence of hydrogen bonded water molecules in the complex.

The ^1H NMR spectrum of **1** displayed a downfield shift in the N—CH_3 resonance signals compared to uncomplexed Tmtu (3.21 ppm vs 3.08 ppm), which is related to an increase in π electron density at the C—N bond upon coordination. In the ^{13}C NMR spectrum of **1**, the main change brought by complexation is the shifting of the C═S resonance towards the upfield region (180.80, 192.78 *vs* 193.42 ppm in Tmtu). The appearance of two resonances could be tentatively explained by considering equilibration of the complex in solution with some other species such as $[Pt(Tmtu)_2(CN)_2]$, **2** (*vide infra*). The N—CH_3 resonances appeared at 43.90 and 42.77 ppm (42.05 ppm for the free ligand). The observation of the cyanide carbon atom signal at 121.79 ppm confirms the coordination of cyanide.

In order to check the plausible intermediacy of mononuclear complex **2**, the reaction was also carried out in the inverse order for the addition of reagents. Under these conditions complex **2** was not detected but the same product **1** was obtained together with traces of a new bridged dinuclear complex **3** (Scheme 1). This compound displays three well resolved peaks in the IR spectrum at 2122, 2134 and 2181 cm^{-1}, as well as a broad weak signal centered around 2250 cm^{-1}, which are attributable to the four different cyanide groups and assigned by comparison to data from theoretical calculations (*vide infra*), and a intense broad signal centered at 1563 cm^{-1} due to the C—N stretching. In the ^1H NMR spectrum of **3** a complex signal in the range 3.25–3.40 ppm was attributed to coordinated Tmtu moieties, whereas the remaining singlet at 3.08 ppm was assigned to an uncomplexed Tmtu molecule and confirmed by increase of the signal upon addition of that reagent. The appearance of four signals in the C═S region of the ^{13}C NMR spectrum at 194.1, 186.7, 186.3 and 184.6 ppm, and four N—CH_3 resonances at 44.5, 44.4, 44.3 and 43.2 ppm (only two peaks attributable to CN resonances can be scarcely recognized above noise at 125.1 and 123.3 ppm) provides additional evidence supporting the proposed structure of complex **3**. Furthermore, the HRMS (positive mode) confirms the existence of the $(M+1)^+$ ion for **3** (m/z = 891.1653 a.m.u.) with isotopic pattern in perfect agreement with the calculated one (see Fig. S2).

X-ray structure description

The molecular structure of compound **1** is shown in Fig. 1. Selected bond lengths and bond angles are given in Table 1. The structure of **1** consists of a divalent cationic complex, $[Pt(Tmtu)_4]^{2+}$ and two crystallographically independent $[Pt(CN)_4]^{2-}$ anions (A and B), each of which resides on a center of symmetry (thus there are two half anions in the asymmetric unit). In $[Pt(CN)_4]^{2-}$, the PtC_4 coordination unit is strictly planar due to an inversion center at the Pt atom for both anions A and B. In $[Pt(Tmtu)_4]^{2+}$, the platinum atom lies within the S_4 plane (deviation ~0.001 Å). The bond angles around Pt^{2+} (the average *cis* and *trans* angles being 90.29° and 171.9° respectively) show some distortion from the regular square planar geometry due to steric constraints of the large Tmtu molecules. The Pt—C≡N moiety is nearly linear with an average bond angle of 177.8°. The carbon atoms in the N—C═S moieties of the ligands are sp^2-hybridized. The Pt—S, Pt—C and other bond distances are in accordance with those reported for related complexes [11]. Most likely, the existence of the complex in the ionic form, $[Pt(Tmtu)_4]^{2+}[Pt(CN)_4]^{2-}$ is due to the high stability of $[Pt(CN)_4]^{2-}$ complex ion in the solid state.

Four O atoms corresponding to water molecules of crystallization were found in the cell, but their hydrogen atoms could not

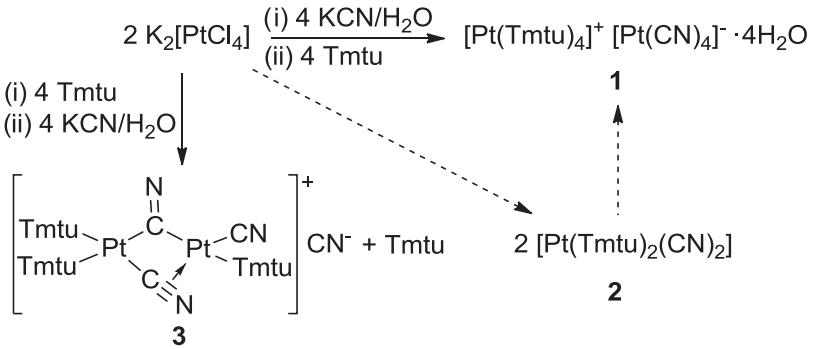

Scheme 1. Synthesis of complexes **1** and **3** and possible intermediate **2**.

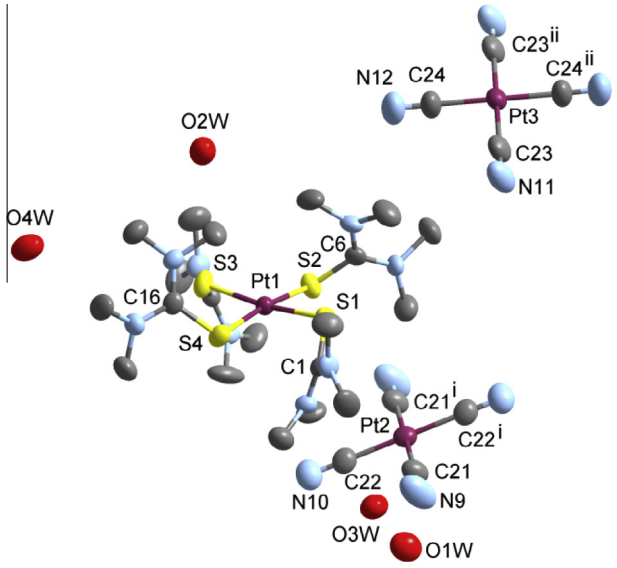

Fig. 1. Molecular structure of $[Pt(Tmtu)_4][Pt(CN)_4]\cdot 4H_2O$ (**1**), with displacement ellipsoids drawn at the 50% probability level (symmetry codes: (i) $-x+1, -y+1, -z+1$; (ii) $-x+1, -y+2, -z$). Hydrogen atoms are omitted.

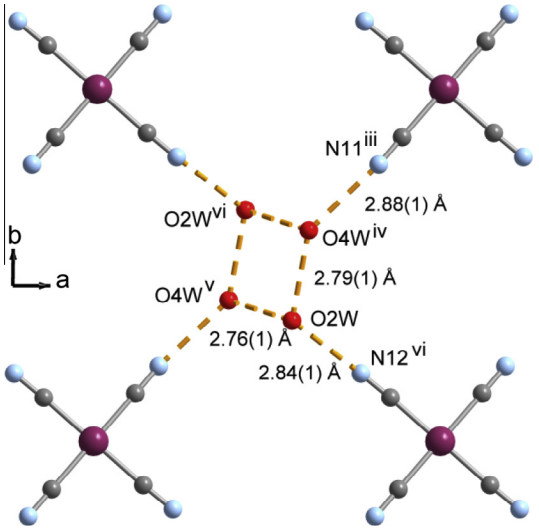

Fig. 2. Hydrate structure of one of the symmetry-independent, albeit similar water tetramers in compound **1**. H-bonds are depicted as dashed orange lines. Above and below this water tetramer only methyl groups from the Tmtu ligands are found. Symmetry transformations: iii = $1+x, y, z$; iv = $x, 1+y, z$; v = $2-x, -y, -z$; vi = $2-x, 1-y, -z$. (For interpretation of the references to colour in this figure legend, the reader is referred to the web version of this article.)

Table 1
Selected bond distances (Å) and bond angles (°) for compound **1**.

Bond distance		Bond angle	
Pt1—S1	2.312(2)	S1—Pt1—S2	90.33(8)
Pt1—S2	2.315(2)	S1—Pt1—S3	171.94(9)
Pt1—S3	2.309(2)	S1—Pt1—S4	89.77(8)
Pt1—S4	2.316(2)	S2—Pt1—S3	90.33(8)
Pt2—C21	1.978(10)	S2—Pt1—S4	171.86(9)
Pt2—C22	1.976(11)	S3—Pt1—S4	90.99(8)
Pt3—C23	1.998(12)	C21—Pt2—C22	91.9(4)
Pt3—C24	1.977(10)	C21—Pt2—C22^{i}	88.1(4)
N9—C21	1.126(12)	C23—Pt3—C24	89.5(4)
N10—C22	1.155(12)	C23—Pt3—C24^{ii}	90.5(4)
N11—C23	1.131(13)	Pt1—S1—C1	109.1(3)
N12—C24	1.141(13)	Pt1—S2—C6	109.4(1)
		Pt1—S3—C11	109.0(8)
		Pt1—S4—C16	111.2(3)

Symmetry transformations: i = $1-x, 1-y, 1-z$; ii = $1-x, 2-y, -z$.

be located, as expected for a room temperature structure. These water molecules are arranged in a tetramer around an inversion center with possibly *homodromic* hydrogen bonds, that is, the H-bonds within the tetramer are arranged in only one clockwise or anticlockwise direction [12]. The second H atom on each water molecule is then pointing to the N atom of a cyanido ligand on the $[Pt(CN)_4]^{2-}$ anions. There are two symmetry independent water tetramers, one built from O1, O3 and the other one built from O2, O4 (Fig. 2). The O···O distances shown in the water substructure lie within the normal range of 2.6–3.0 Å found for other examples of water clusters in coordination structures [13].

Theoretical calculations

Quantum chemical calculations were undertaken at the DFT level (see Computational Details) in order to gain insight into the process leading to the final formation of compound **1** and its structural features. First of all the plausible intermediate formation of a mononuclear $[Pt(Tmtu)_2(CN)_2]$ species **2** was evaluated. At the *C* level of theory, the *cis*-**2** isomer was found to be 1.20 kcal/mol more stable than *trans*-**2**. The cationic ($\mathbf{1}^{cat}$) and anionic ($\mathbf{1}^{ani}$) constituents of the ion-pair **1** were also separately computed at the same level and the model reaction $\mathbf{2} \rightarrow \frac{1}{2}\mathbf{1}^{cat} + \frac{1}{2}\mathbf{1}^{ani}$ was found to be endergonic by 3.64 kcal/mol at the *B* level of theory. To take into consideration the interactions within the ion-pair framework, the minimum energy structure for the dinuclear (homocoordinated) system $\mathbf{1}^{calc}$ (without water molecules) was calculated, as well as the dimeric homodinuclear (heterocoordinated) structure $\mathbf{2}_2$ (Fig. 3). The energetic of this further elaborated model reaction $\mathbf{2}_2 \rightarrow \mathbf{1}^{calc}$ was then computed and found to be exergonic by 8.18 kcal/mol (*B* level), which explains the experimentally observed preference in the solid state. The energy difference is high enough to rule out the possibility of observing $\mathbf{2}_2$ in NMR experiments. The above mentioned NMR signal splitting should rather be explained by differentiation of two sets of proximal and distal Tmtu ligands with respect to the anionic component in the close ion pair **1**.

Analysis of bond strength parameters for Pt-Do (Do, donor atoms) bonds has been shown to be useful for the study of related complex systems [14]. Relevant data for all computed species are collected in Table 2. A first general observation is that Wiberg bond indices (WBIs) [15] fail to correlate when comparing mononuclear – having too small values – with dinuclear complexes. Ion pair $\mathbf{1}^{calc}$ formation from the mononuclear ionic constituents ($\mathbf{1}^{cat}$ and $\mathbf{1}^{ani}$) seems to have negligible effect in the Pt-Do distances, although a small but significant strengthening is observed for the Pt—C bonds. The overall natural charge transfer from the anionic to the cationic unit in $\mathbf{1}^{calc}$ was found to be 0.020 au.

The minimum energy arrangement in the homodinuclear $\mathbf{2}_2$ system locates the $Pt1(CN)_2$ moiety close and (roughly) orthogonally oriented with respect to the $Pt2(Tmtu)_2$ unit, thus spatially enabling the required internuclear ligand exchange for affording **1**. Worth is to mention a general (average) weakening of Pt—C bonds in $\mathbf{2}_2$ along with (average) strengthening of Pt—S bonds. A possible explanation for this fact arises from the observed intermolecular noncovalent interactions (in addition to hydrogen bonding) between two N atoms belonging to the cyanide ligands at the Pt1 center with one of the S atoms attached to the other Pt2 center (Fig. 4). These interactions are located at roughly contact distances ($d_{N\cdots S}$ = 3.304 and 3.696 Å; $WBI_{N\cdots S}$ = 0.009 and 0.003), close to the sum of van der Waals radii, and evidenced by the existence of the

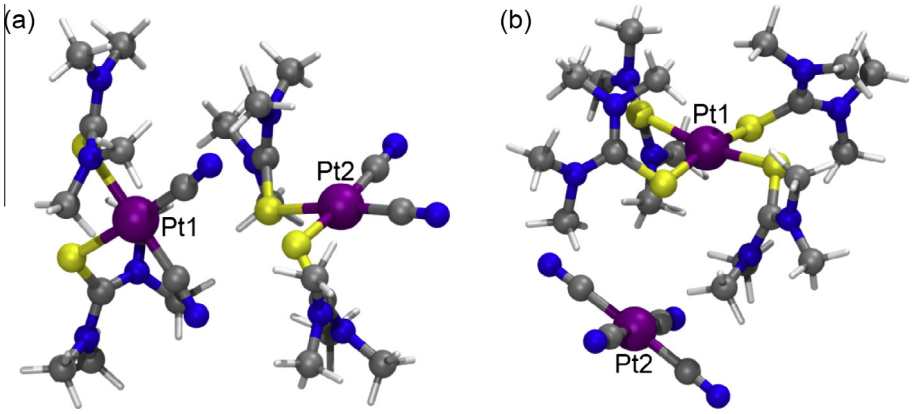

Fig. 3. Calculated (level A) structures for dinuclear species (a) $\mathbf{2}_2$ and (b) $\mathbf{1}^{calc}$.

Table 2
Metal–ligand bond distances (Å) and bond-strength related parameters in mono- and dinuclear computed (*B* level) complexes.[a]

		$\mathbf{1}^{cat}$	$\mathbf{1}^{ani}$	***cis*-2**	$\mathbf{1}^{calc}$	$\mathbf{2}_2$	**3**
Pt-C	d_{Pt-C}		2.012	1.972	2.012	1.979	1.918 2.150, 2.157 1.973, 2.361
	WBI_{Pt-C}		0.539	0.649	0.757	0.775	0.849 0.458, 0.433 0.688, 0.207
	MBO_{Pt-C}		0.808	0.878	0.827	0.883	1.000 0.514, 0.532 0.703, 0.305
	$\rho(\mathbf{r})_{Pt-C}$[b]		13.84	15.18	13.85	14.95	17.23 10.05, 9.86 14.84, 6.07
Pt-S	d_{Pt-S}	2.365		2.471	2.364	2.406	2.337
	WBI_{Pt-S}	0.468		0.364	0.675	0.617	0.718
	MBO_{Pt-S}	0.707		0.693	0.715	0.682	0.826
	$\rho(\mathbf{r})_{Pt-S}$[b]	9.63		7.76	9.67	8.85	10.39

[a] Average values, except for Pt-C bonds in **3**, for which the bonds of CN groups a–c (lines 1–3, respectively) with Pt1 (left) and Pt2 (right) are separately collected.
[b] In 10^{-2} *e* a_0^{-3}.

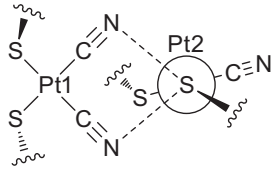

Fig. 4. Sketched representation of complex $\mathbf{2}_2$ viewed in Newman projection along a S-Pt2 bond axis.

respective bond critical points ($\rho(\mathbf{r})_{N\cdots S} = 0.83 \cdot 10^{-2}$ and $0.52 \cdot 10^{-2}$ *e* a_0^{-3}). The NBO method allows analysis of interactions between filled donor and virtual acceptor orbital spaces, within the NBO basis, for the study of either inter or intramolecular interactions [16]. Estimation of such donor–acceptor interactions by second order perturbation theory analysis of Fock matrix, points to an intermolecular interaction within $\mathbf{2}_2$ largely dominated by electron flow from slightly populated antibonding Pt1—CN bonds to empty Rydberg-type orbitals at the S atom attached to Pt2, with associated stabilizing energies of 12.36 and 9.65 kcal/mol for every single interaction. Consequently, decrease of the electron density at Pt1—CN bonds increases their bond strength (WBI and MBO), whereas the increase of electron density at the involved S_{Pt2} atom contributes to a remarkable strengthening of that particular Pt—S_{Pt2} bond ($d_{Pt2-S} = 2.392$ Å; $WBI_{Pt2-S} = 0.629$; $MBO_{Pt2-S} = 0.704$; $\rho(\mathbf{r})_{Pt2-S} = 9.15 \cdot 10^{-2}$ *e* a_0^{-3}) with respect to the average and to the monomer *cis*-**2**. An overall (natural) charge transfer of 0.011 au has been estimated from the Pt1 to the Pt2 units.

The most stable van der Waals complex between **3** and Tmtu was also found to be much less stable than $\mathbf{1}^{calc}$ by 19.26 kcal/mol at the working level of theory, which justifies that **3** is formed either transiently or, more likely, as a minor side product. Complex **3** features two different platinum centres connected by two different cyanido bridging units, one is a roughly symmetric μ^2-CN (unit "b") whereas the other is an asymmetric μ^2-η^2-CN (unit "c") (Fig. 5), with the central Pt_2C_2 core significantly folded (C(b)—Pt1—Pt2—C(c) dihedral = 114.7°). One more terminal CN ligand (unit "a") is coordinated to Pt2, the three remaining coordination sites around the roughly square planar Pt centres being occupied by Tmtu ligands. The most weekly bound Tmtu ligand (compare with average values in Table 2) is the one located *trans* to μ^2–η^2–CN at Pt1 ($d_{S1-Pt1} = 2.380$ Å; WBI = 0.646; MBO = 0.757; $\rho(\mathbf{r}) = 9.51 \cdot 10^{-2}$ *e* a_0^{-3}). The overall cationic $[Pt_2(CN)_3(Tmtu)_3]^+$ unit in **3** is electrically compensated by one free cyanide anion (unit "d). The four different CN units (a–d) in the calculated structure **3**, with predicted unscaled stretching frequencies at 2116.3 (unit "c"), 2142.0 ("b"), 2152.7 ("d") and 2236.4 cm^{-1} ("a"), are in good agreement with the experimentally observed IR spectrum (*vide supra*).

Antimicrobial activity

The antimicrobial activities (average of three measurements) of free Tmtu ligand, the platinum(II) complex **1** and Amoxil (as a

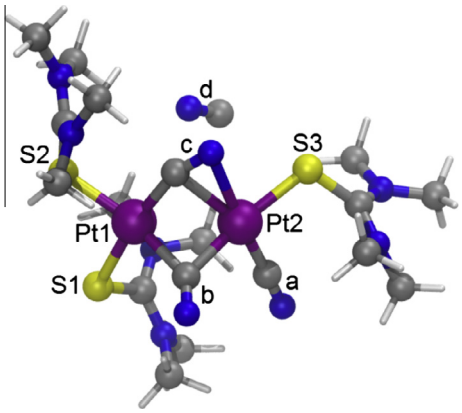

Fig. 5. Calculated (level A) structure for complex **3**, showing the numbering scheme for Pt and S atoms, as well as for all four different CN groups (a–d).

Table 3
Antimicrobial activities evaluated by the minimum inhibitory concentration (MIC: μg mL^{-1}).

	E.c.[a]	P.a.[b]	A.n.[c]	P.c.[d]	C.a.[e]	S.c.[f]
Amoxil	8	12	890	870	660	580
Tmtu	50	30	140	90	250	210
1	370	320	540	470	610	>1000

[a] *Escherichia coli*.
[b] *Pseudomonas aeruginosa*.
[c] *Aspergillus niger*.
[d] *Penicillium citrinum*.
[e] *Candida albicans*.
[f] *Saccharomyces cerevisiae*.

Table 4
Crystal and refinement data for complex **1**.

Formula	$C_{24}H_{56}N_{12}O_4Pt_2S_4$
Formula weight	1095.23
Crystal system	Triclinic
Space group	*P*−*1*
a, *b*, *c* (Å)	10.3490(2), 10.5480(2), 19.2708(5)
α, *β*, *γ* (deg.)	85.2720(10), 89.1110(10), 89.3220(10)
V (Å^3)	2096.10(8)
Z	2
ρ (calcd.) (g cm^{-3})	1.735
μ (Mo Kα) (mm^{-1})	6.908
Crystal Size (mm)	0.23 × 0.06 × 0.1
F(000)	1072
θ range (deg.)	1.06–25.25
h, *k*, *l* limits	−12:12, −12:11, −23:23
Max., Min. trans.	0.820, 0.2995
Reflections: collected, unique	31677, 7500 (R_{int} = 0.0385)
Observed data [$I > 2\sigma$ (I)]	6119
Nref, Npar	7500, 434
R_1, wR_2, S[$I > 2\sigma$ (I)][a]	0.0393, 0.0861, 1.126
R_1, wR_2, (all data)	0.542, 0.891
Largest diff. peak, hole (e/Å^{-3})	1.688, −1.500

[a] $w = [\sigma^2(F_o^2) + (0.0165P)^2 + 18.1526P]^{-1}$ where $P = (F_o^2 + 2F_c^2)/3$.

standard drug) evaluated by minimum inhibitory concentrations (MIC; μg mL^{-1}) are listed in Table 3. Complex **1** showed significant activity against two gram-negative bacteria (*Escherichia coli, Pseudomonas aeruginosa aeruginosa*). Moderate activity was observed against the studied molds (*Aspergillus niger, Penicillium citrinum*) and a yeast (*Candida albican*). A comparative study shows that ligand Tmtu is more effective than complex **1**. In general, the biological activity of complexes could be attributed to whether or not they possess the tendency to undergo ligand replacement with the biological ligands such as proteins and DNA [17]. This suggests that Pt in the title complex is not so labile for easy ligand displacement by biological ligands. This robustness is due to the fact that both ligands, cyanide and Tmtu, are strongly bound to the soft Pt(II) ion (see Table 2) and they are not prone to be easily dissociated, thus resulting in a poor activity, in comparison with previously reported weakness of Pt—Cl bonds [18].

Conclusions

The present study describes the crystal structure as well as theoretical validation of a novel platinum-cyanide-tetramethylthiourea complex. The major product in both two synthetic sequences tested is a heterodinuclear Pt(II) ion pair complex **1** constituted by a $[Pt(Tmtu)_4]^{2+}$ cation and a $[Pt(CN)_4]^{2-}$ anion. It crystallizes with four water molecules exhibiting *homodromic* hydrogen bonding and possesses moderate activity against a variety of microorganisms. A minor product **3** was also obtained in one of the synthetic sequences.

DFT calculations give support to the thermodynamic stability of complex **1** in comparison to a isomeric dimer of homonuclear complex *cis*-$[Pt(Tmtu)_2(CN)_2]$, *cis*-**2**, which could be a precursor of **1**. Complex **3** (after taking Tmtu into the energetic balance) turned out to be much less stable than **1** and *cis*-$\mathbf{2_2}$ and features a remarkable Pt(II) heterodinuclear $[(Tmtu)_2Pt(\mu^2\text{-}CN)\text{-}(\mu^2\text{-}\eta^2\text{-}CN)Pt(Tmtu)(CN)]^+ CN^-$ ionic structure with four different CN units and a folded Pt_2C_2 core.

Experimental section

General comments

Potassium tetrachloridoplatinate(II), K_2PtCl_4 was obtained from Strem Chemical Company, USA and tetramethylthiourea (Tmtu) was purchased from Acros Organics, Belgium. IR spectra were recorded on Perkin–Elmer FTIR 180 spectrophotometer using KBr pellets over the range 4000–500 cm^{-1}. The ^{1}H and ^{13}C NMR spectra in DMSO-d_6 or $CDCl_3$ were obtained on a Jeol JNM-LA 500 NMR or a Bruker AV600 spectrometers operating at frequencies of 500.00 MHz and 600.00 MHz respectively, at 297 K for proton nuclei and at frequencies of 125.65 MHz and 150 MHz, with ^{1}H broadband decoupling at 298 K, for carbon nuclei. Chemical shifts were referred to tretamethylsilane or the residual peak from the deuterated solvent. Mass spectrometry was recorded on HPLC-MS TOF 6220 instrument. The antimicrobial activities (average of three measurements) of free ligand, the platinum(II) complex 1 and Amoxil (as a standard drug) were estimated by minimum inhibitory concentrations (MIC; μg mL^{-1}) as described earlier [9]. Standard culture media of bacteria, *E. coli*, (ATCC 13706) and *P. aeruginosa* (MTCC 424), and molds, *A. niger* (MTCC 1349) and *P. citrinum* (MTCC 5215) and yeast *C. albicans* (MTCC 183) and *Saccharomyces cerevisiae* (MTCC 463) were obtained from Qingdao Yijia Huuyi Co. China.

*Synthesis of complex **1***

The title complex was prepared by reaction of $K_2[PtCl_4]$, KCN and Tmtu. 0.415 g (1 mmol) $K_2[PtCl_4]$ in 10 mL water was mixed with 2 equivalents of KCN in 10 mL water and after stirring the clear red colour solution for half an hour, 0.265 g (2 mmol) Tmtu in 10 mL methanol was added. Upon addition of Tmtu the red colour of the solution turned to light reddish orange. The solution was stirred for half an hour and then it was filtered. The filtrate was kept for crystallization on slow evaporation. Dark yellow crystals were obtained, which were washed with methanol and dried. Yield 50%, M.p 195–196 °C. Anal. Calc: C, 26.32%; H, 5.15%; N, 15.35%; S, 11.71%. Found: C, 26.40%; H, 4.96%; N, 14.95%; S, 11.48%. IR (ν, cm^{-1}) 3400 (br), 2128 (s), 1561(s), 607 (m). ^{1}H NMR (500 MHz, DMSO, ppm) δ 3.21 (s,12H); ^{13}C NMR (125 MHz, DMSO, ppm) δ 42.77, 43.90, 121.79, 180.80, 192.78.

Synthesis of complex 3·Tmtu

To a stirred solution of 0.1 g of $K_2[PtCl_4]$ (0.24 mmol) in 10 mL of water at room temperature, 0.064 g of Tmtu (0.48 mmol) were added. After 30 min, 0.031 g of KCN (0.48 mmol) were added and the resulting mixture was refluxed overnight. The reaction was cooled to room temperature and extracted with dichloromethane. The organic layer was dried over anhydrous Na_2SO_4 and the solvent evaporated under reduced pressure to obtain a yellow solid. Yield 15%. IR (ν, cm^{-1}) 2250 (br w), 2181, 2134, 2122, 1563 (s). ^{1}H NMR (600 MHz, $CDCl_3$, ppm) δ 3.08 (s,12H), 3.25–3.40 (m,36H); ^{13}C NMR (150 MHz, $CDCl_3$, ppm) δ 43.2, 44.3, 44.4, 44.5, 123.3, 125.1, 184.6, 186.3, 186.7, 194.1. HRMS-(*m*/*z*) for $C_{19}H_{37}N_{10}S_3Pt_2$, calculated: 891.1648, found: 891.1653 $(M + H)^+$.

X-ray structure determination

The X-ray data for **1** were collected on a Bruker SMART APEX-II CCD diffractometer using graphite monochromated MoKα radiation (λ = 0.71073 Å) at 296 K. SAINT was used for the cell refinement and data reduction [19]. The structure was solved by applying the direct method using SHELXS-97 and refined by a full-matrix least-squares calculation on F^2 using SHELXL-97 [20]. For molecular graphics PLATON [21] was used. H atoms on crystal water molecules were neither found nor calculated but are included in the formula, formula weight, density and $F(000)$. Crystal data and details of the data collection are given in Table 4. CCDC-1028968 contains the supplementary crystallographic data for this paper. These data can be obtained free of charge from The Cambridge Crystallographic Data Centre via www.ccdc.cam.ac.uk/data_request/cif.

Computational details

Quantum chemical calculations were performed with the ORCA electronic structure program package [22]. All geometry optimizations were run with tight convergence criteria using the B3LYP [23] functional together with the new efficient RIJCOSX algorithm [24] and the def2-TZVP basis set [25]. The [SD(60,MWB)] effective core potential (ECP) was used for Pt atoms [26]. In all optimizations and energy evaluations, the latest Grimme's semiempirical atom-pairwise correction, accounting for the major part of the contribution of dispersion forces to the energy, was included [27]. Solvent effects (DMSO) were taken into account via the COSMO solvation model [28]. From these geometries computed at the above mentioned level (*A* level), all reported data were obtained, unless otherwise stated, by means of single-point (SP) calculations using the same functional as well as the more polarized def2-TZVPP [25,29,30] basis set (*B*-level). Bond strengths were characterized by the Mayer Bond Order (MBO) [31] or Wiberg Bond Index (WBI) [15], the later derived from the natural bond orbital (NBO) population analysis [32]. The topological analysis of the electronic charge density, $\rho(\mathbf{r})$, within Bader's Atoms-In-Molecules (AIM) methodology [33] was conducted using the AIM2000 software [34]. Reported energies are uncorrected for the zero-point vibrational term. Energy in Tmtu and mononuclear complexes was evaluated at a higher level using the very extense and polarized def2-QZVPP basis set (*C* level) [25,35]. Figs. 3 and 5 were generated with VMD [36].

Acknowledgment

J.R. wishes to thank the Spanish Ministerio de Economía y Competitividad and FEDER (Project SAF2011-26611) for financial support.

Appendix A. Supplementary material

Supplementary data associated with this article can be found, in the online version, at http://dx.doi.org/10.1016/j.molstruc.2014.12.076.

References

[1] (a) S.V. Zutphen, J. Reedijk, Coord. Chem. Rev. 24 (2005) 2845–2853;
(b) D. Wong, S.J. Lippard, Nat. Rev. Drug Disc. 4 (2005) 307–320;
(c) Y. Jung, S.J. Lippard, Chem. Rev. 107 (2007) 1387–1407;
(d) S. Ahmad, Chem. Biodiv. 7 (2010) 543–566.
[2] S. Ahmad, A.A. Isab, S. Ali, Transition Met. Chem. 31 (2006) 1003–1016.
[3] (a) M. Kartalou, J.M. Essigmann, Mutat. Res. 478 (2001) 23–43;
(b) D.J. Stewart, Crit. Rev. Oncol. Hematol. 63 (2007) 12–31.
[4] J. Reedijk, Chem. Rev. 99 (1999) 2499–2510.
[5] (a) M. Green, M. Garner, D.M. Orton, Transition Met. Chem. 17 (1992) 164–176;
(b) Z. Guo, P.J. Sadler, Angew. Chem. Int. Ed. 38 (1999) 1512–1531.
[6] (a) G. Marverti, M. Cusumano, A. Ligabue, M.L. Di Pietro, P.A. Vainiglia, A. Ferrari, M. Bergomi, M.S. Moruzzi, C. Frassineti, J. Inorg. Biochem. 102 (2008) 699–712;
(b) L. Fuks, E. Anuszewska, H. Kruszewska, A. Krowczynski, J. Dudek, N. Sadlej-Sosnowska, Transition Met. Chem. 35 (2010) 639–647.
[7] P.A. Gale, M.E. Light, R. Quesada, Cryst. Eng. Comm. 8 (2006) 178–188.
[8] (a) R.L. Girling, K.K. Chatterjee, E.L. Amma, Inorg. Chim. Acta 7 (1973) 557–562;
(b) F. Bachechi, L. Zambonelli, G. Marcotrigiano, J. Chem. Crystallogr. 7 (1977) 11–20;
(c) J. Arpalahti, B. Lippert, H. Schollhorn, U. Thewalt, Inorg. Chim. Acta 153 (1988) 51–55;
(d) U. Bierbach, T.W. Hambley, N. Farrell, Inorg. Chem. 37 (1988) 708–716;
(e) A.N. Westra, C. Esterhuysen, K.R. Koch, Acta Cryst. C 60 (2004) m395–m398;
(f) J. Calvo, J.S. Cases, E. Garcia-Martinez, Y. Parajo, A. Sanchez-Gonzalez, J. Sordo, Z. Anorg, Allg. Chem. 630 (2004) 215–216;
(g) M. Mizota, Y. Yokoyama, K. Sakai, Acta Cryst. E 61 (2005) m1433–m1435;
(h) J. Lin, G. Lu, L.M. Daniels, X. Wei, J.B. Sapp, Y. Deng, J. Coord. Chem. 61 (2008) 2457–2469.
[9] M.R. Malik, V. Vasylyeva, K. Merz, N. Metzler-Nolte, M. Saleem, S. Ali, A.A. Isab, K.S. Munawar, S. Ahmad, Inorg. Chim. Acta 376 (2011) 207–211.
[10] C.L. Exstrom, M.K. Pomije, K.R. Mann, Chem. Mater. 10 (1998) 942–945.
[11] (a) F. Bachechi, L. Zambonelli, G. Marcotrigiano, J. Chem. Crystallogr. 7 (1977) 11–12;
(b) U. Bierbach, T.W. Hambley, N. Farrell, Inorg. Chem. 37 (1998) 708–716;
(c) C. Mühle, J. Nuss, R.E. Dinnebier, M. Jansen, Z. Anorg, Allg. Chem. 630 (2004) 1462–1468;
(d) K. Sakai, M. Mizota, N. Akiyama, Acta Cryst. E 60 (2004) m88–m90;
(e) B.A. Maynard, R.E. Sykora, Acta Cryst. E 64 (2008) m138–m139.
[12] C. Janiak, T.G. Scharmann, W. Günther, F. Girgsdies, H. Hemling, W. Hinrichs, D. Lentz, Chem. Eur. J. 1 (1996) 637–644.
[13] (a) C. Janiak, T.G. Scharmann, K.-W. Brzezinka, P. Reich, Chem. Ber. 128 (1995) 323–328;
(b) C. Janiak, T.G. Scharmann, H. Helmling, D. Lentz, J. Pickardt, Chem. Ber. 128 (1995) 235–244;
(c) C. Janiak, T.G. Scharmann, S.A. Mason, J. Am. Chem. Soc. 124 (2002) 14010–14011;
(d) J.P. Naskar, M.G.B. Drew, A. Hulme, D.A. Tocher, D. Datta, CrystEngComm 7 (2005) 67;
(e) Q.-Y. Liu, X. Li, CrystEngComm 7 (2005) 87;
(f) Y.Q. Sun, J. Zhang, Z.F. Ju, G.Y. Yang, Aust. J. Chem. 58 (2005) 572;
(g) F. Zhuge, B. Wu, J. Liang, J. Yang, Y. Liu, C. Jia, C. Janiak, N. Tang, X.-J. Yang, Inorg. Chem. 48 (2009) 10249–10256.
[14] (a) J. Ruiz, V. Rodríguez, C. de Haro, A. Espinosa, J. Pérez, C. Janiak, Dalton Trans. (2010) 3290–3301;
(b) J Ruiz, V. Rodríguez, N. Cutillas, A. Espinosa, M.J. Hannon, J. Inorg. Biochem. 105 (2011) 525–531;
(c) J. Ruiz, C. Vicente, C. de Haro, A. Espinosa, Inorg. Chem. 50 (2011) 2151–2158;
(d) J. Ruiz, V. Rodríguez, N. Cutillas, A. Espinosa, M.J. Hannon, Inorg. Chem. 50 (2011) 9164–9171;
(e) J. Ruiz, V. Rodríguez, N. Cutillas, K.G. Samper, M. Capdevila, O. Palacios, A. Espinosa, Dalton Trans. 41 (2012) 12847–12856;
(f) A. Zamora, V. Rodríguez, N. Cutillas, G.S. Yellol, A. Espinosa, K.G. Samper, M. Capdevila, O. Palacios, J. Ruiz, J. Inorg. Biochem. 128 (2013) 48–56.
[15] K. Wiberg, Tetrahedron 24 (1968) 1083–1096.
[16] A.E. Reed, L.A. Curtiss, F. Weinhold, Chem. Rev. 88 (1988) 899–926.
[17] S. Ahmad, A.A. Isab, S. Ali, A.R. Al-Arfaj, Polyhedron 25 (2006) 1631–1643.
[18] For instance, $\rho(r) = 7.91\cdot10^{-2}\ e\ a_0^{-3}$ for the Pt-Cl bond in [Pt(ET-dmba)Cl(PTA)] (ET-dmba = 17-α-[4′-ethinyl-dimethylbenzylamine]-17-β-testosterone; PTA = 1,3,5-triaza-7-phosphaadamantane) (see Ref. 14b) or $\rho(r) = 7.78\cdot10^{-2}\ e\ a_0^{-3}$ for [Pt(ppy)Cl(1C3)] (ppy = 2-phenylpyridine; 1C3 = 1-[(3-aminopropyl) amino]-anthracene-9,10-dione) (see ref. 14c).
[19] Bruker. APEX2 and SAINT. Bruker AXS Inc., Madison, Wisconsin, USA, 2007.
[20] G.M. Sheldrick, Acta Cryst. A 64 (2008) 112–122.
[21] A.L. Spek, Acta Cryst. D 65 (2009) 148–155.
[22] ORCA - An *ab initio*, DFT and semiempirical SCF-MO package. Written by F. Neese, Max Planck Institute for Bioinorganic Chemistry, D-45470 Mülheim/Ruhr, 2012. Version 2.9.1. <http://www.cec.mpg.de/forum/portal.php>.
[23] (a) A.D. Becke, J. Chem. Phys. 98 (1993) 5648–5652;
(b) C.T. Lee, W.T. Yang, R.G. Parr, Phys. Rev. B 37 (1988) 785–789.
[24] F. Neese, F. Wennmohs, A. Hansen, U. Becker, Chem. Phys. 356 (2009) 98–109.
[25] F. Weigend, Phys. Chem. Chem. Phys. 7 (2005) 3297–3305.
[26] D. Andrae, U. Häussermann, M. Dolg, H. Stoll, H. Preuss, Theor. Chim. Acta 77 (1990) 123–141. ECP parameters for Pt [SD(60,MWB)] were obtained from the pseudopotential library of the Stuttgart/Cologne group, <http://www.theochem.uni-stuttgart.de/pseudopotentials/>.
[27] S. Grimme, J. Antony, S. Ehrlich, H. Krieg, J. Chem. Phys. 132 (2010) 154104.
[28] (a) A. Klamt, G. Schüürmann, J. Chem. Soc. Perkin Trans. 2 (220) (1993) 799–805;
(b) A. Klamt, J. Phys. Chem. 99 (1995) 2224–2235.
[29] A. Schäfer, C. Huber, R. Ahlrichs, J. Chem. Phys. 100 (1994) 5829–5835.

[30] D. Feller, J. Comp. Chem. 17 (1996) 1571–1586. Basis sets may be obtained from the Basis Set Exchange (BSE) software and the EMSL Basis Set Library: <https://www.bse.pnl.gov/bse/portal>.
[31] (a) I. Mayer, Chem. Phys. Lett. 97 (1983) 270–274;
(b) I. Mayer, Int. J. Quant. Chem. 26 (1984) 151–154;
(c) I. Mayer, Theor. Chim. Acta 67 (1985) 315–322;
(d) I. Mayer, in: Z.B. Maksic (Ed.), Modelling of Structure and Properties of Molecules, John Wiley & Sons, New York, Chichester, Brisbane, Toronto, 1987;
(e) A.J. Bridgeman, G. Cavigliasso, L.R. Ireland, J. Rothery, J. Chem. Soc., Dalton Trans. (2001) 2095–2108
[32] (a) A.E. Reed, F. Weinhold, J. Chem. Phys. 78 (1983) 4066–4073;
(b) A.E. Reed, R.B. Weinstock, F. Weinhold, J. Chem. Phys. 83 (1985) 735–746. Using the NBO 5.9 code. E.D. Glendening, J.K. Badenhoop, A.E. Reed, J.E. Carpenter, J.A. Bohmann, C.M. Morales, F. Weinhold, Theoretical Chemistry Institute, University of Wisconsin, Madison, 2001.
[33] (a) R.F.W. Bader, Atoms in Molecules: A Quantum Theory, Oxford University Press, Oxford, 1990;
(b) R.F.W. Bader, Chem. Rev. 91 (1991) 893–928;
(c) C.F. Matta, R.J. Boyd, in: C.F. Matta, R.J. Boyd (Eds.), The Quantum Theory of Atoms in Molecules, Wiley-VCH, New York, 2007, pp. 1–34.
[34] (a) F. Biegler-König, J. Schönbohm, D. Bayles, J. Comp. Chem. 22 (2001) 545–559 (AIM2000 v. 2.0, designed by F. W. Biegler-König, and J. Schönbohm, (2002). Home page <http://www.aim2000.de/>);
(b) F. Biegler-König, J. Schönbohm, J. Comp. Chem. 23 (2002) 1489–1494.
[35] A. Schäfer, C. Huber, R. Ahlrichs, J. Chem. Phys. 119 (2003) 12753–12762.
[36] W. Humphrey, A. Dalke, K. Schulten, J. Mol. Graphics 14 (1996) 33–38. <http://www.ks.uiuc.edu/Research/vmd/>.